


Cytotoxic Activity of the Mesoionic Compound MIH 2.4BI in Breast Cancer Cell Lines

Breast Cancer: Basic and Clinical Research
Volume 14: 1–14
© The Author(s) 2020
Article reuse guidelines:
sagepub.com/journals-permissions
DOI: 10.1177/1178223420913330



Luciana Amaral de Mascena Costa^{1,2}, Ashlyn C Harmon²,
Alvaro Aguiar Coelho Teixeira¹, Filipe Cássio Silva de Lima^{1,2},
Silvany de Sousa Araújo¹, Fabio Del Piero³,
Helivaldo Diógenes da Silva Souza⁴,
Petrônio Filgueiras de Athayde Filho⁴, Severino Alves Junior⁵,
Maria de Mascena Diniz Maia⁶, Aurea Wischral⁷,
Manoel Adrião Gomes Filho¹ and J Michael Mathis^{2,8} 

¹Department of Morphology and Animal Physiology, Federal Rural University of Pernambuco, Recife, Brazil. ²Department of Comparative Biomedical Sciences, School of Veterinary Medicine, Louisiana State University, Baton Rouge, LA, USA. ³Department of Pathobiological Sciences, School of Veterinary Medicine, Louisiana State University, Baton Rouge, LA, USA. ⁴Department of Chemistry, Federal University of Paraíba, João Pessoa, Brazil. ⁵Department of Fundamental Chemistry, Federal University of Pernambuco, Recife, Brazil. ⁶Department of Biology, Federal Rural University of Pernambuco, Recife, Brazil. ⁷Department of Veterinary Medicine, Federal Rural University of Pernambuco, Recife, Brazil. ⁸Graduate School of Biomedical Sciences, University of North Texas Health Science Center, Fort Worth, TX, USA.

ABSTRACT: In this work, we report the synthesis of a new 1,3-thiazolium-5-thiolate derivative of a mesoionic compound (MIH 2.4BI) and the characterization of its selective cytotoxicity on a panel of breast cancer cell lines. The cytotoxic effect of MIH 2.4BI on breast cancer cell lines was determined by XTT and crystal violet assays, flow cytometry analysis, electron microscopy characterization, and terminal deoxynucleotidyl transferase (TdT) deoxyuridine triphosphate (dUTP) nick end labeling (TUNEL) apoptosis assays. As determined using XTT cell growth and survival assays, MIH 2.4BI exhibited growth inhibition activity on most breast cancer cell lines tested, compared with normal human mammary epithelial cells. Three breast cancer cell lines (MCF-7, T-47D, and ZR-75-1) showed a more potent sensitivity index to growth inhibition by MIH 2.4BI than the other breast cancer cell lines. Interestingly, these 3 cell lines were derived from tumors of Luminal A origin and have ER (estrogen receptor), PR (progesterone receptor), and HER2 (human epidermal growth factor receptor 2) positive expression. Additional analysis of cytotoxicity mediated by MIH 2.4BI was performed using the MCF-7 cell line. MCF-7 cells displayed both time- and dose-dependent decreases in cell growth and survival, with a maximum cytotoxic effect observed at 72 and 96 hours. The MCF-7 cells were also characterized for cell cycle changes upon treatment with MIH 2.4BI. Using flow cytometry analysis of cell cycle distribution, a treatment-dependent effect was observed; treatment of cells with MIH 2.4BI increased the G2/M population to 34.2% compared with 0.1% in untreated (control) cells. Ultrastructural analysis of MCF-7 cells treated with MIH 2.4BI at 2 different concentrations (37.5 and 75 μ M) was performed by transmission electron microscopy. Cells treated with 37.5 μ M MIH 2.4BI showed morphologic changes beginning at 6 hours after treatment, while cells treated with 75 μ M showed changes beginning at 3 hours after treatment. These changes were characterized by an alteration of nuclear morphology and mitochondrial degeneration consistent with apoptotic cell death. Results of a TUNEL assay performed on cells treated for 96 hours with MIH 2.4BI supported the observation of apoptosis. Together, these results suggest that MIH 2.4BI is a promising candidate for treating breast cancer and support further *in vitro* and *in vivo* investigation.

KEYWORDS: Apoptosis, breast cancer, cancer therapy, cell cycle, MCF-7 cells, mesoionic compound

RECEIVED: September 29, 2019. **ACCEPTED:** February 25, 2020.

TYPE: Original Research

FUNDING: The author(s) disclosed receipt of the following financial support for the research, authorship, and/or publication of this article: We acknowledge CAPES (Coordenação de Aperfeiçoamento de Pessoal de Nível Superior) for an international scholarship through the Science without Borders program (88887.122971/2016-00), and research funding from the Louisiana State University School of Veterinary Medicine. These

funders had no role in study design, data collection and analysis, decision to publish, or preparation and submission of the article.

DECLARATION OF CONFLICTING INTERESTS: The author(s) declared no potential conflicts of interest with respect to the research, authorship, and/or publication of this article.

CORRESPONDING AUTHOR: J Michael Mathis, Graduate School of Biomedical Sciences, University of North Texas Health Science Center, 3500 Camp Bowie Boulevard, Fort Worth, TX 76107, USA. Email: michael.mathis@unthsc.edu

Introduction

Breast cancer is the most frequently diagnosed cancer and the leading cause of cancer death in women worldwide, accounting for approximately 24% of all new cancer cases and is the leading cause of cancer death in over 100 countries.¹ The incidence rate of breast cancer has also shown a rise in most transitional countries, particularly in South America, Africa, and Asia, resulting in about 2.1 million newly diagnosed cases estimated

in 2018. Thus, breast cancer is one of the most critical public health problems in the world facing women.

According to the Surveillance, Epidemiology Outcomes Program (SEER) of the National Cancer Institute, 1 in 3 cancers diagnosed in women in the United States is breast cancer.² Despite the early detection methods and advancement of conventional treatments, more than 252 710 new cases of invasive breast cancer were expected to occur among US women in



Creative Commons Non Commercial CC BY-NC: This article is distributed under the terms of the Creative Commons Attribution-NonCommercial 4.0 License (<https://creativecommons.org/licenses/by-nc/4.0/>) which permits non-commercial use, reproduction and distribution of the work without further permission provided the original work is attributed as specified on the SAGE and Open Access pages (<https://us.sagepub.com/en-us/nam/open-access-at-sage>).

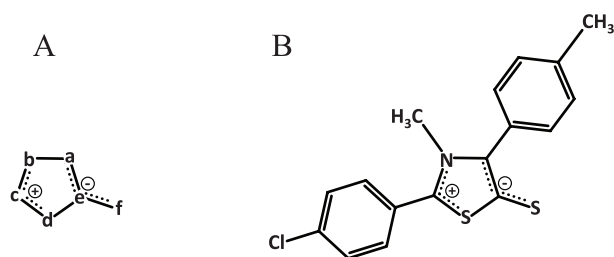


Figure 1. Chemical structure of the mesoionic compounds. (A) Shown is the characteristic of a mesoionic compound containing a heterocyclic ring with carbon and 2 or more heteroatoms (a-e) as well as an exocyclic heteroatom of oxygen, nitrogen, or sulfur (f). The heterocyclic structure is dipolar and has both negative and positive charges that are delocalized. (B) Shown is the structure of the thiazolium-based mesoionic compound, 2-(4-chlorophenyl)-3-methyl-4-(4-methylphenyl)-1,3-thiazolium-5-thiolate (MIH 2.4BI).

2017.² Although breast cancer rates are declining in several countries in Europe and North America over the past 25 years due to early detection methods such as mammography and better treatments, there were still 40 610 estimated deaths for breast cancer among women in the United States in 2017.² While early-stage breast cancer is treated with high success, advanced breast cancer remains difficult to manage due to limitations of currently available treatments. Advanced breast cancer tends to develop resistance to standard therapies, leaving palliative care as the remaining option for these patients. Therefore, new therapies aimed at alternative and complementary strategies are necessary.

There is a growing interest in studying the biological activity of mesoionic compounds,³⁻⁵ which possesses a 5-membered heterocyclic aromatic ring associated with a sextet of electrons (Figure 1A). The heterocyclic ring has a positive charge balanced by a corresponding negative charge located on a covalently attached atom. This characteristic of a mesoionic structure having well-separated regions of positive and negative charges associated with a polyheteroatomic system suggests the capability of mesoionic compounds to have strong interactions with biomolecules such as DNA and proteins. Although these compounds are internally charged, they are also neutral overall and therefore can cross biological membranes. Among the mesoionic compounds, the class of sydnone compounds is distinguished by their biological activities, such as antibacterial, antitumoral, antifungal, antimalarial, analgesic, anti-inflammatory, anticonvulsive, antipyretic, and antiparasitic.⁶

The potential use of these compounds as chemotherapeutic agents has been investigated mainly for treating melanoma.^{7,8} These studies involving a new 1,3,4-thiadiazolium indicated that this mesoionic compound was able to inhibit the transport of electrons through the respiratory chain system between complexes II and III, collapsing the transmembrane and stimulating ATPase activity in intact mitochondria. These effects related to mitochondrial energy appeared to be associated with changes in membrane permeability and fluidity.⁸ Sydnone

compounds containing a 1,2,3-oxadiazole core with a keto group in the 5 position. A series of sydnone derivatives were synthesized by Dunkley and Thoman.⁹ In a screening assay of a cancer cell line panel, including MCF-7, NCI-H460, and SF-268 cells, an N-(4'-F-3'-nitrophenyl) sydnone exhibited cytotoxic activity against all 3 cell lines.⁹ The anticancer activity of another sydnone compound, sydnone 1 (SYD-1), was tested *in vitro*¹⁰ and *in vivo* in the context of a rat Walker-256 carcinosarcoma model.¹¹ Treatment of rats with SYD-1 decreased tumor volume and tumor weight compared with untreated animals. An investigation of the mechanism of action of SYD-1 suggested that the anticancer activity of mesoionic compounds might be related to changes in mitochondrial metabolism and activation of apoptotic pathways, leading to tumor cell death.¹⁰ These results confirm the potential role of mesoionic compounds as anticancer agents in the treatment of several types of cancer.

Given these considerations, we report the synthesis of a 1,3-thiazolium-5-thiolate mesoionic compound (MIH 2.4BI). In this study, we examined the potential for selective cancer killing by MIH 2.4BI using a panel of breast cancer cell lines and cells derived from normal human breast lineage. Treatment with MIH 2.4BI resulted in an inhibition of cell growth and survival in most of the breast cancer cell lines tested, compared with normal human mammary epithelial cells (HMECs). In particular, MCF-7 cells displayed both time- and dose-dependent decreases in cell growth and survival, with a maximum cytotoxic effect by MIH 2.4BI observed at 72 and 96 hours. MCF-7 cells treated with MIH 2.4BI demonstrated an alteration in cell cycle distribution, resulting in an increased G2/M subpopulation compared with the cell cycle distribution of untreated (control) cells. In addition, morphologic changes consistent with apoptotic cell death were identified in MCF-7 cells treated with MIH 2.4BI, a finding confirmed by the results of a terminal deoxynucleotidyl transferase (TdT) deoxyuridine triphosphate (dUTP) nick end labeling (TUNEL) apoptosis assay used to detect apoptotic DNA fragmentation. Together, these results support further *in vitro* and *in vivo* investigation of MIH 2.4BI as a potential breast cancer therapeutic.

Materials and Methods

Synthesis of MIH 2.4BI

All reagents and solvents for the synthesis of MIH 2.4BI were purchased from commercial sources (Sigma-Aldrich; São Paulo, Brazil) and used without further purification. For the synthesis of the free base mesoionic compound, MIH 2.4BI was synthesized from N-methyl-C-4-methylphenylglycine and N-(4-chlorobenzoyl)-N-methyl-C-4-methylphenylglycine as follows.

For the synthesis of N-methyl-C-4-methylphenylglycine, the following method was used.¹² First, 250 mmol of potassium cyanide (KCN), 250 mmol of methylammonium hydrochloride,

and 100 mL of water were combined. The mixture was stirred with the addition of approximately 250 mmol of 4-methylbenzaldehyde previously diluted in 100 mL of methanol. After 4 hours of vigorous stirring, about 150 mL of distilled water was added, and the solution was extracted with toluene (3×100 mL). The toluene phase was collected in a flask and concentrated on a rotary evaporator. Then, 300 mL of 6M HCl was added, and the solution was subjected to reflux. After 6 hours of reflux, about 70% of the 6M HCl was evaporated under reduced pressure to give the amino acid (in hydrochloride form), and the resulting crystals were filtered. Then, the crystals were washed with solvent (dichloromethane or chloroform) to remove any yellowish impurities. The amino acid obtained was purified by recrystallization from ethanol:water (1:1), and white crystals were obtained; 214–217°C m.p. and 64% yield. $^1\text{H-NMR}$ ($\text{DMSO-}d_6$): 2.27 (s, 3H); 2.37 (s, 3H); 4.96 (s, 1H); 7.24 (d, 2H); 7.36 (d, 2H), and 9.64 (s, 2H in NH_2^+).

For the synthesis of N-(4-chlorobenzoyl)-N-methyl-C-(4-methylphenyl)glycine, the following method was used.¹³ First, 8.63 mmol of the N-methyl-C-(4-methylphenyl)glycine was dissolved in 30 mL of 10% NaOH in an Erlenmeyer flask and left under mechanical stirring for 2 hours. While under stirring, 8.63 mmol of 4-chlorobenzoyl chloride was added and left an additional 2 hours. The reaction mixture was then neutralized with concentrated HCl and extracted with chloroform (3×100 mL). The chloroform phase was concentrated under reduced pressure, providing a sticky white mass. The final product was purified by recrystallization from ethanol/water (1:1), and white crystals were obtained; 152–154°C m.p. $^1\text{H-NMR}$ (CDCl_3): 2.34 (s, 3H); 2.70 (s, 3H); 6.34 (s, 1H); 7.18 (d, 2H); 7.23 (d, 2H); 7.62 (d, 2H); 8.22 (d, 2H).

For the final synthesis of the MIH 2.4Bl mesoionic compound 2-(4-chlorophenyl)-3-methyl 4-(4-methylphenyl)-1,3-thiazolium-5-thiolate, the following method was used.¹⁴ First, 3.14 mmol of N-(4-chlorobenzoyl)-N-methyl-C-4-methylphenylglycine was dissolved in 10 mL of acetic anhydride, and the reaction mixture was allowed to warm to 60°C for 1 hour. After that, the reaction was cooled, and 20 mL of CS_2 was added. A red solution was formed, which was refluxed at 65°C for an additional 1 hour. The reaction mixture was then allowed to stand at room temperature for 48 hours. Subsequently, a solution of methanol/distilled water (1:1) was added until the mixture became cloudy. After 24 hours of standing, a precipitate was obtained as red crystals. The product was filtered and air-dried, and red crystals were obtained; 188–190°C m.p. and 51% yield. IV (KBr, cm^{-1}): 3041, 3007 ($\text{C}_{\text{Ar}}-\text{H}$); 2991, 2972 ($\text{C}-\text{H}$); 1587, 1483 ($\text{C}=\text{N}$ and C_{Ar}), 1290 ($\text{C}-\text{S}$); 1093 ($\text{C}_{\text{Ar}}-\text{Cl}$); 831 ($\text{C}_{\text{Ar}}-\text{H}$). $^1\text{H-NMR}$ ($\text{DMSO-}d_6$): 2.37 (s, 3H, CH_3); 3.58 (s, 3H, CH_3); 7.32 (d, 2H, $J=8.0$ Hz, CH_{Ar}); 7.49 (d, 2H, $J=8.1$ Hz, CH_{Ar}); 7.69 (d, 2H, $J=8.6$ Hz, CH_{Ar}); 7.77 (d, 2H, $J=8.6$ Hz, CH_{Ar}). $^{13}\text{C-NMR}$ ($\text{DMSO-}d_6$): 159.95, 151.20, 140.00, 138.10, 136.17, 131.37, 130.99, 129.41, 128.88, 127.55, 125.87, 40.88, 20.96. The final red MIH 2.4Bl crystal product was dissolved in dimethyl sulfoxide (DMSO) for experimental use.

Cells lines and culture of cells

The characteristics of the human and mouse cell line used for the cytotoxicity assays are shown in Table 1, as described by Smith et al.¹⁵ All cell lines were obtained from the American Type Culture Collection (ATCC; Manassas, Virginia). The breast cancer cell lines were cultured in Dulbecco's modified Eagle medium (DMEM, Genesee Scientific; San Diego, California) supplemented with 10% fetal bovine serum (FBS, Gemini Bio-Products; West Sacramento, California), 1% non-essential amino acids (Gemini Bio-Products), and 1% antibiotic/antimycotic solution (Gemini Bio-Products) containing 100 IU (international units)/mL penicillin, 100 $\mu\text{g}/\text{mL}$ streptomycin, and 25 $\mu\text{g}/\text{mL}$ amphotericin B. Mammary Epithelial Cell Basal Medium (ATCC) was used for the culture of the HMECs supplemented with a Mammary Epithelial Cell Growth Kit (ATCC) containing 5 $\mu\text{g}/\text{mL}$ hH-insulin, 6 mM L-glutamine, 0.5 μM epinephrine, 5 $\mu\text{g}/\text{mL}$ apo-transferrin, 5 ng/mL recombinant human (rH)-transforming growth factor- α (TGF- α), 0.4% ExtractP, and 100 ng/mL hydrocortisone hemisuccinate. The MCF-10A cells were cultured in DMEM/Ham's F12 media supplemented with 5% Equine Serum (Gemini Bio-Products), 20 ng/mL epidermal growth factor (EGF) (Sigma-Aldrich; St. Louis, Missouri), 10 $\mu\text{g}/\text{mL}$ insulin (Sigma-Aldrich), 0.5 mg/mL hydrocortisone (Sigma-Aldrich), 100 ng/mL cholera toxin (Sigma-Aldrich), and 1% antibiotic/antimycotic solution. All cell lines were cultured at 37°C with 5% CO_2 under a humidified atmosphere condition.

Crystal violet cytotoxicity assay

For the evaluation of changes in relative cell growth and survival after treatment with MIH 2.4Bl, a crystal violet assay¹⁶ was used. The crystal violet assay is a simple nonspecific dye that is directly proportional to the number of viable adherent cells. Cells were initially seeded 24 hours into 96-well tissue culture plates at a density of 5×10^3 per well. Subsequently, the cells were treated with the MIH 2.4Bl mesoionic compound using 8 increasing concentrations: 1.2, 2.3, 4.7, 9.4, 18.8, 37.5, 75, and 150 μM . As a positive control, cells were treated with doxorubicin at 1.34 μM , a concentration representing approximately $10 \times$ the reported IC_{50} (half maximal inhibitory concentration) in MCF-7 cells.^{17–19} As a negative control, cells were treated with vehicle (DMSO) alone at 0.1% (v/v) in media. The cells were treated at each concentration using 8 replicate wells for 24, 48, 72, and 96 hours. At each time point, the media was removed, and the wells were washed twice with Dulbecco's phosphate-buffered saline solution (PBS). Afterward, the plates were gently inverted on filter paper to remove any remaining liquid and dried at room temperature. The dried cells were fixed and stained with 20% methanol containing 0.5% w/v crystal violet. Each plate was briefly rinsed with water, and the plates were allowed to dry. After the addition of 200 μL of 95% ethanol/40 mM HCl to solubilize the crystal violet stained cells, the optical density (OD) of each

Table 1. Classification and basic expression profile of a panel of normal and breast cancer cell lines.

CELL LINE	TUMOR TYPE	HISTOLOGICAL CLASSIFICATION	RECEPTOR STATUS			SPECIES
			ER	PR	HER2	
4T1	AC	Basal-like	–	–	–	Mouse (BALB/c)
BT-20	C	Basal A	–	–	+	Human
BT-549	DC	Basal B	–	–	–	Human
MCF7	AC	Luminal A	+	+	–	Human
MDA-MB-231	AC	Basal B	–	–	–	Human
MDA-MB-436	AC	Basal B	–	–	–	Human
MM2MT	AC	Unknown	Unknown	Unknown	Unknown	Mouse (BfC3H)
T-47D	DC	Luminal A	+	+	+	Human
ZR-75-1	DC	Luminal A	+	+	+	Human
HMEC	N	Normal breast	+	+	–	Human
MCF-10A	F	Normal breast	–	–	–	Human
MM3MG	N	Normal breast	Unknown	Unknown	Unknown	Mouse (BALB/c)

Abbreviations: AC, adenocarcinoma; C, carcinoma; DC, ductal carcinoma; ER, estrogen receptor; F, fibrocystic disease; HER2, human epidermal growth factor receptor 2; HMEC, human mammary epithelial cell; N, normal breast, PR, progesterone receptor.

well at 595 nm was measured using a plate reader (SpectraMax 190, Molecular Devices; San Jose, California).

XTT cytotoxicity assay

Changes in relative cell growth and survival after treatment with MIH 2.4Bl were confirmed with the use of an XTT assay (Cell Signaling Technology; Danvers, Massachusetts). The XTT assay is based on the reduction of a colorless tetrazolium salt to a colored formazan product due to the activity of mitochondrial dehydrogenases in the mitochondria of living cells. Cells were initially plated for 24 hours in 96-well tissue culture plates at a density of 5×10^3 per well. Subsequently, the cells were treated with the MIH 2.4Bl mesoionic compound using 8 increasing concentrations: 1.2, 2.3, 4.7, 9.4, 18.8, 37.5, 75, and 150 μ M. As a positive control, the cells were treated with doxorubicin at 1.34 μ M, a concentration representing approximately $10 \times$ the reported IC_{50} in MCF-7 cells.¹⁷⁻¹⁹ As a negative control, cells were treated with vehicle (DMSO) alone at 0.1% (v/v) in media. The cells were treated at each concentration using 8 replicate wells for 24, 48, 72, and 96 hours. At each time point, the plates were subjected to the following treatment: 50 μ L of XTT detection solution (a 1:50 ratio of electron coupling solution to XTT Reagent) was added to each well containing 200 μ L media. After a 2-hour incubation at 37°C, the OD of each well at 595 nm was measured using a SpectraMax 190 plate reader (Molecular Devices; San Jose, California).

Flow cytometric analysis of cell cycle

For cell cycle analysis, MCF-7 cells were initially seeded for 24 hours into 6-well tissue culture plates at a density of 1.0×10^5 cells per well. Subsequently, the cells were treated with MIH 2.4Bl at 75 μ M for 0, 1, 3, 6, 12, and 24 hours. As a negative control, cells were treated with vehicle (DMSO) alone at 0.1% (v/v) in media for 24 hours. At each time point, the cells were harvested and fixed in 70% ice-cold ethanol. After the cells were stained with propidium iodide, DNA content was analyzed by flow cytometry as previously described.²⁰ The percentage of cells in each cell cycle phase was calculated using the ModFit LT software (version 3.2; Verity Software House, Brunswick, Maine) based on DNA histograms of 20 000 cells per treatment.

Transmission electron microscopy

The MCF-7 cell line was used for the transmission electron microscopy (TEM) characterization. The cells were initially plated into 10 mm round coverslips (Thermanox, Nunc; Rochester, New York) that were coated with 0.1% poly-L-lysine solution (w/v) in H₂O and placed into 12-well plates. The wells were seeded with 2×10^5 cells/well and cultured for 24 hours. Subsequently, the cells were treated with the MIH 2.4Bl mesoionic compound at 2 different concentrations (37.5 and 75 μ M). As a control, the cells were also treated with DMSO (vehicle) alone. The cells were treated at each

concentration for 3, 6, 9, 12, and 24 hours. To perform the TEM analysis at each time point, the coverslips were washed with PBS, and the cells were fixed with 1.6% paraformaldehyde/2.6% glutaraldehyde at room temperature for 2 hours. Afterward, the coverslips were washed 3 times for 10 minutes with H₂O, placed into a 2% osmium contrast staining solution for 1 hour, and washed again 3 times for 10 minutes each with H₂O. The cells were then dehydrated with graded ethanol at 30%, 50%, and 70% for 5 minutes each, followed by 80%, 90%, and 100% ethanol 2 times for 10 minutes each. The coverslips were embedded in Epon Resin 828 (Hexion; Columbus, Ohio) and sectioned. The sections were subsequently stained for 30 minutes with 2% aqueous uranyl acetate, followed by staining with 0.5% aqueous lead citrate. The stained sections were imaged on a Jeol JEM-1400 120 kV TEM instrument (JEOL; Peabody, Massachusetts), and images were captured on a CMOS camera (Gatan; Pleasanton, California).

TUNEL assay

Apoptosis was determined using a TUNEL method using a Click-iT Plus EdU Alexa Fluor 594 Imaging Kit (Thermo Fisher Scientific; Waltham, Massachusetts). MCF-7 cells were initially seeded overnight into Nunc Lab-Tek 8 well chamber slides at a density of 20 000 cells/well. Subsequently, the cells were treated with MIH2.4BI at 37.5 or 75 μ M for 96 hours. As a negative control, cells were treated with vehicle (DMSO) alone. Afterward, the cells were washed 2 times in PBS. The cells were then fixed for 15 minutes at room temperature in 4% paraformaldehyde. The cells were then permeabilized using 0.25% Triton X-100 in PBS for 20 minutes and washed twice with deionized water. For the TUNEL reaction, 100 μ L of TdT reaction cocktail containing TdT reaction buffer, EdUTP, and TdT were added to each well, and the cells were incubated for 60 minutes at 37°C. Afterward, the wells were washed twice with 3% bovine serum albumin (BSA) in PBS for 5 minutes each. Subsequently, 50 μ L of the Click-iT™ Plus TUNEL reaction cocktail was added to each well and incubated for 30 minutes at 37°C, protected from light. Each well was then washed twice with 3% BSA in PBS for 5 minutes. The cells were counterstained with ActinGreen™ 488 ReadyProbes® Reagent (Thermo Fisher) and DAPI (4',6-diamidino-2-phenylindole), and imaged by fluorescence microscopy on a Nikon TE2000-U inverted microscope.

Statistical analysis

The cell growth and survival data were calculated from the mean OD readings obtained for each concentration of the MIH 2.4BI mesoionic compound assayed normalized to the mean OD readings of the negative (no treatment) control and mean blank (no cell) values and were expressed as mean percentage values with standard error (SEM). For the comparison between the breast cancer cell lines and the HMECs, a

one-way analysis of variance (ANOVA) was applied, followed by Dunnett's post hoc test (used for pairwise analysis between a set of treatments against a single control mean). Data were considered statistically significant when $P < .05$. Cytotoxicity was expressed as mean IC₅₀ (concentration that inhibits 50% of cell growth and survival over negative control) of the cell lines as determined using a nonlinear regression analysis in the GraphPad Prism software (version 7.0; La Jolla, California), SEM and confidence intervals (95% CI) calculated from the curves. The mean percent inhibition values were plotted against the MIH 2.4BI concentrations allowing for the generation of a sigmoidal dose-response curve using the following equation: $Y = 100 / (1 + 10^{(X - \text{LogIC}_{50}) \times \text{HillSlope}})$. The IC₅₀ values were obtained by the interpolation of curve-fit data from each curve using the GraphPad Prism software. An extra sum-of-squares F test was also used to evaluate the differences in the curve-fit parameters among the data sets using the GraphPad Prism software. A one-way ANOVA analysis was also used to determine significant differences among treatments, followed by a Dunnett's post hoc test to compare all pairs of data sets. Data were considered statistically significant when $P < .05$.

Results

Assessment of cytotoxicity

The effect of thiazolium-based mesoionic compounds in breast cancer cells has not been examined. We chose to focus on the MCF-7 cell line because it is one of the most widely used cell lines as a model for hormone-receptor positive breast cancer both in vitro and in vivo.²¹ The MCF-7 cell line retains several characteristics of a differentiated mammary epithelium,²² and its characterization includes detailed transcriptome analysis.^{23,24} In addition, the extensive body of published literature on MCF-7 cells provides contextual relevance in studying breast cancer biology and drug development.^{21,22}

Initially, to examine the cytotoxic effect of MIH 2.4BI in the MCF-7 breast cancer cell line, we compared the crystal violet assay with another commonly used assay using the XTT (2,3-bis-(2-methoxy-4-nitro-5-sulfophenyl)-2h-tetrazolium-5-carboxanilide) reagent (Figure 2). The dose-response curves presented in Figure 2 indicate that MIH 2.4BI decreased MCF-7 cell growth and survival, as determined by either XTT or crystal violet assay. To assess IC₅₀ values, the dose-response curves were analyzed using a 4-parameter logistic regression model, with a variable slope that allows nonlinear fitting of the Hill coefficient. The results of this analysis showed that the half-maximal inhibition concentration (IC₅₀) for MIH 2.4BI was 65.3 μ M for the crystal violet assay and 68.7 μ M for the XTT assay (Table 2). Importantly, a statistical comparison of the dose-response curves in Figure 2 indicates that the XTT and crystal violet assays demonstrated no statistical difference between the curve-fit values ($P = .87$).

Although the XTT assay is a commonly used method to determine cytotoxic effects in cells, it may not be reliable when

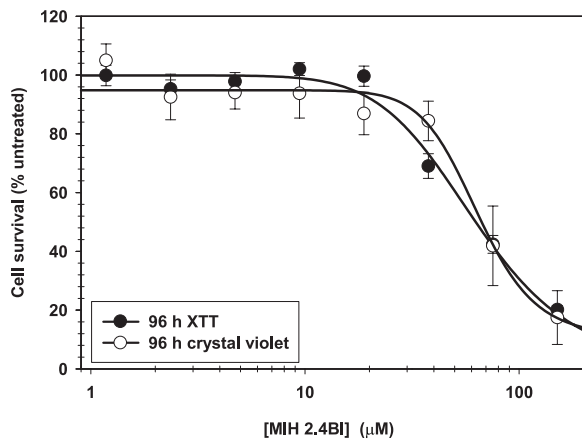


Figure 2. Effect of MIH 2.4BI on growth and survival of the MCF-7 breast cancer cell line. The relative cell growth and survival was determined by XTT (●) and crystal violet (○) assays after 96 hours of incubation. Each point represents the mean \pm SEM performed in replicates of 8. The IC_{50} values were calculated from the best fit of the Hill slope curve to experimental data using a nonlinear regression analysis. IC_{50} indicates half maximal inhibitory concentration.

Table 2. IC_{50} values obtained by treatment of MCF-7 cells for 96 hours with MIH 2.4BI.

ASSAY	96 HOURS		
	IC_{50} (μ M)	95% CI (μ M)	R^2
Crystal violet	65.3	59.2-72.2	0.91
XTT	68.7	54.3-87.0	0.60

Abbreviations: IC_{50} , half maximal inhibitory concentration; 95% CI, 95% confidence interval; R^2 , goodness of fit.

comparing across different cell lines and time points due to potential variations in metabolic capacity.^{25,26} Therefore, we used the crystal violet assay to analyze the effects of MIH 2.4BI in MCF-7 cells (Figure 3) and a panel of breast cancer cell lines and cells of normal human breast lineage (Figure 4), based on the simplicity of the assay and its suitability for examining the impact of chemotherapeutics on cell growth and survival and growth inhibition.¹⁶

Further analysis of cytotoxicity mediated by MIH 2.4BI was performed at various concentrations and treatment time points using the MCF-7 cell line. As shown in Figure 3, MCF-7 cells exhibited a time-dependent decrease in cell growth and survival by treatment with MIH 2.4BI from 24 to 96 hours. At the highest concentration tested (150 μ M), there was no significant difference observed between the cytotoxic effect at the 72- and 96-hour treatment time points (Figure 3). A dose-dependent decrease in cell growth and survival from treatment using MIH 2.4BI was also observed, and the IC_{50} values were calculated at each time point from the nonlinear regression curves. As summarized in Table 3, the calculated IC_{50} values were 155.5, 86.1, 53.3, and 65.3 μ M at 24, 48, 72, and 96 hours of treatment, respectively. A comparison of the 4

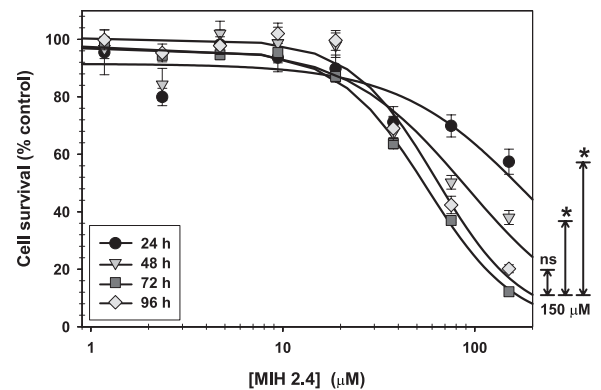


Figure 3. Dose-dependent effect of MIH 2.4BI on growth and survival of the MCF-7 breast cancer cell line. MCF-7 cells were treated with increasing concentrations of MIH 2.4BI for 24 (●), 48 (▼), 72 (■), or 96 hours (◆). Relative cell growth and survival was determined at each time point by XTT assays. Each point represents the mean \pm SEM of data performed in replicates of 8. Calculated at 150 μ M, inhibition of cell growth and survival at 24, 48, and 72 hours were significantly different than 96 hours if $P < .05$ (*). ns indicates not significant.

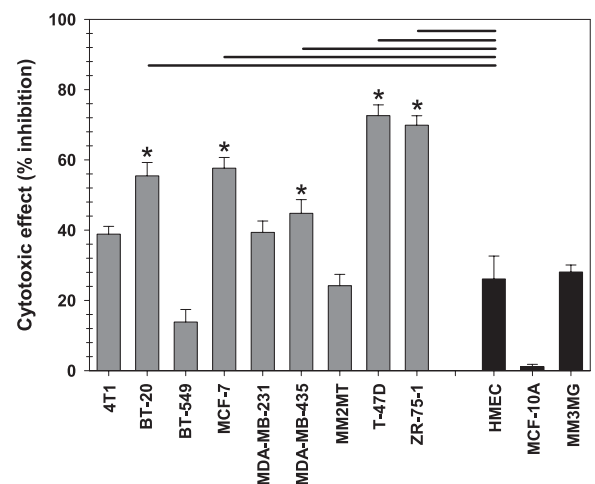


Figure 4. Cytotoxic effect of MIH 2.4BI on a panel of breast cancer cell lines. Percent inhibition of cell growth and survival was determined by XTT assay after treatment for 72 or 96 hours with 75 μ M MIH 2.4BI. Calculated at 96 hours, inhibition of breast cancer cell lines were statistically greater than normal HMECs if $P < .05$ (*). HMEC indicates human mammary epithelial cell.

dose-response curves using an extra sum-of-squares F test indicated statistically significant differences between the curve-fit values ($P < .0001$).

We next compared the cytotoxic effect of MIH 2.4BI in a panel of breast cancer cell lines (4T1, BT-20, BT-549, MCF-7, MDA-MB-231, MDA-MB-436, MM2MT, MM3MG, T-47D, and ZR-75-1) and compared the effect in cells of normal human breast lineage (HMEC and MCF-10A). To assess the cytotoxicity of MIH 2.4BI in different cell lines, we used the crystal violet staining assay (Figure 4). In this assay, 1×10^3 cells were seeded into 96-well tissue culture plates and treated for 96 hours with a single concentration of MIH 2.4BI at 75 μ g/mL or with vehicle (DMSO) alone.

Table 3. IC₅₀ values obtained by treatment of MCF-7 cells for 24 to 96 hours with MIH 2.4BI.

TIME	IC ₅₀ (μM)	95% CI (μM)	R ²
24	155.5	128.9-187.6	0.90
48	86.1	77.0-96.3	0.94
72	53.3	51.8-54.9	0.99
96	65.3	62.2-68.6	0.98

Abbreviations: IC₅₀, half maximal inhibitory concentration; 95% CI, 95% confidence interval; R², goodness of fit.

Table 4. Percent inhibition of breast cancer cell lines and normal breast epithelial cells treated with 75 μM of MIH 2.4BI for 96 hours.

CELL LINE	% INHIBITION (MEAN ± SEM)
4T1	38.8 ± 2.2
BT-20	55.4 ± 3.8
BT-549	13.8 ± 3.6
MCF-7	57.6 ± 3.0
MDA-MB-231	39.4 ± 3.2
MDA-MB-436	44.8 ± 3.9
MM2MT	24.2 ± 3.3
MM3MG	28.0 ± 2.0
T-47D	72.6 ± 3.1
ZR-75-1	69.9 ± 2.7
HMEC	26.1 ± 6.5
MCF-10A	1.1 ± 0.6

Abbreviation: HMEC, human mammary epithelial cell.

As shown in Figure 4 and summarized in Table 4, the different cell lines displayed various levels of cytotoxic inhibition mediated by MIH 2.4BI at 96-hour treatment. The data were evaluated according to an intensity scale²⁷ that was used to assess the cytotoxic potential of the MIH 2.4BI. This scale classified response in different cell lines as no activity (1% to 20% inhibition), little activity (inhibition ranging from 20% to 50%), moderate activity (inhibition ranging from 50% to 70%), and high activity (inhibition of growth ranging from 70% to 100%). After analyzing the data presented in Table 4, we observed that MIH 2.4BI inhibited cell growth and survival in most of the breast cancer cell lines, varying between no activity (BT-549), little activity (4T1, MDA-MB-231, MDA-MB-436, MM2MT, and MM3MG), moderate activity (BT-20 and MCF-7), and high activity (T-47D and ZR-75-1). It is worth noting that 5 breast cancer cell lines (BT-20, MCF-7, MDA-MB-436, T-47D, and ZR-75-1) demonstrated a significantly higher

growth inhibitory activity than normal HMECs at 96-hour treatment (Figure 4). Importantly, MCF-10A (a spontaneously immortalized nontumorigenic cell line derived from benign proliferative breast tissue) showed no inhibitory activity from treatment with MIH 2.4BI, while normal HMECs showed only a slight inhibitory activity (Figure 4).

As shown in Table 5, the IC₅₀ values for the cancer cell lines were less than the values for the HMECs at 48 (148.0 μM), 72 (193.8 μM), and 96 hours (133.0 μM), except for 3 cell lines. In general, the BT-20, BT-549, and MM2MT cell lines demonstrated less sensitivity to MIH 2.4BI than the other breast cancer cell lines. In contrast, 3 breast cancer cell lines (MCF-7, T-47D, and ZR-75-1) displayed a more potent sensitivity to growth inhibition by MIH 2.4BI compared with HMEC at 72 and 96 hours of treatment than the other breast cancer cell lines. Interestingly, the MCF-7, T-47D, and ZR-75-1 cell lines were derived from tumors of luminal A origin and have ER (estrogen receptor), PR (progesterone receptor), and HER2 (human epidermal growth factor receptor 2) positive expression.

We determined the selectivity index (SI) of MIH 2.4BI, a mathematical ratio of the IC₅₀ values of the treatment in HMECs to the IC₅₀ values of the treatments in each of the cancer cell lines. An SI value ≥2.0 is considered to have a significant selectivity,²⁸ such that the treatment is more than twice as cytotoxic to the cancer cell line as compared with the normal cell line. In contrast, an SI value of <2 is considered to give general cell toxicity in both cancer and normal cells. As shown in Table 6, we observed that treatment with MIH 2.4BI for 96 hours was more selective for MCF-7 (2.0-fold), T-47-D (4.4-fold), and ZR-75-1 (3.5-fold) than for HMEC.

Cell cycle analysis

To further characterize the effects of MIH 2.4BI in breast cancer cells, we examined the effect of MIH 2.4BI on cell cycle using flow cytometry analysis. As shown in Figure 5, we observed a treatment-dependent effect of MIH 2.4BI on cell cycle distribution. Treatment of cells with MIH 2.4BI resulted in an increase in the G2/M population to 34.2% (Figure 5B) compared with 0.1% in untreated (control) cells (Figure 5A). This increase of the cell population at the G2/M phase was accompanied by a time-dependent decrease of the cell population in the G1 and S phases of the cell cycle (Figure 5C). In contrast, untreated cells demonstrated no significant changes in cell cycle distribution over 24 hours (data not shown).

Transmission electron microscopy

To correlate cytotoxic effects on inhibition of cell growth and survival, we examined morphological changes in MCF-7 cells treated with MIH 2.4BI. The cells were initially treated with a moderate dose of 37.5 μM MIH 2.4BI for 3, 6, 12, and 24 hours (Figure 6). Ultrastructural analysis of control and DMSO (vehicle)-treated MCF-7 cells revealed that

Table 5. Comparison of IC₅₀ values obtained by treatment of normal and breast cancer cells with MIH 2.4BI.

CELL LINE	48 HOURS			72 HOURS			96 HOURS		
	IC ₅₀	95% CI	R ²	IC ₅₀	95% CI	R ²	IC ₅₀	95% CI	R ²
	(μ M)	(μ M)		(μ M)	(μ M)		(μ M)	(μ M)	
4T1	NC	NC	NC	122.4	113.8-131.7	0.92	102.7	97.8-108.0	0.96
BT-20	217.0	168.3-279.9	0.67	126.5	114.2-140.3	0.86	81.9	75.7-88.8	0.91
BT-549	190.9	147.9-246.4	0.47	NC	NC	NC	167.6	150.3-186.9	0.84
MCF-7	70.3	53.9-91.8	0.85	49.7	46.5-53.2	0.99	54.2	48.1-61.1	0.95
MDA-MB-231	102.1	89.9-116.0	0.79	67.1	60.4-74.5	0.91	86.3	82.6-90.5	0.97
MDA-MB-436	127.0	114.8-140.4	0.84	111.5	106.6-116.6	0.96	81.1	73.3-89.8	0.89
MM2MT	154.7	147.4-162.4	0.93	110.8	104.9-117.0	0.95	170.4	148.8-195.1	0.80
MM3MG	139.2	132.4-146.4	0.93	117.5	111.3-124.1	0.95	124.3	119.4-129.4	0.97
T-47D	111.6	72.3-172.4	0.47	63.5	52.9-76.2	0.83	30.2	27.0-33.9	0.93
ZR-75-1	93.4	67.2-129.9	0.36	68.1	53.9-86.0	0.63	38.3	33.9-43.2	0.92
HMEC	148.0	84.95-257.9	0.48	193.8	97.52-385.3	0.20	133.0	105.9-167.1	0.65
MCF-10A	106.6	101.6-111.9	0.96	126.6	120.7-132.8	0.96	152.6	149.2-156.1	0.92

Abbreviations: 95% CI, 95% confidence interval; R², goodness of fit; NC, nonconvergence of data using the nonlinear regression analysis.

Table 6. Values for the SI.

CELL LINE	48 HOURS	72 HOURS	96 HOURS
4T1	NT	1.6	1.3
BT-20	0.7	1.5	1.6
BT-549	0.8	NT	0.8
MCF7	1.7	3.6	2.0
MDA-MB-231	1.4	2.9	1.5
MDA-MB-436	1.2	1.7	1.6
MM2MT	1.0	0.6	1.3
T-47D	1.3	3.1	4.4
ZR-75-1	1.6	2.8	3.5

Abbreviations: HMEC, human mammary epithelial cell; IC₅₀, half maximal inhibitory concentration; NT, not tested (representing the tumor lines with data that did not converge in the IC₅₀ analysis); SI, selectivity index. SI was calculated by determining the ratio of the IC₅₀ value of normal HMECs divided by the IC₅₀ value of the breast cancer cell line.

regardless of the evaluation time point, their morphology was rounded with a prominent rather euchromatic nucleus and with some regions of heterochromatin. Numerous mitochondria were observed in the cytoplasm (Figure 6A-D) of control and vehicle-treated cells. MCF-7 cells treated with 37.5 μ M MIH 2.4BI revealed changes only beginning at the 6-hour post-treatment time point; at 3 hours after initiation of treatment, no morphologic changes were observed compared with control or vehicle-treated cells (data not shown).

The changes observed at 6-hour treatment with MIH 2.4BI were defined by altered nuclear morphology (Figure 6E) and the presence of numerous autophagic cytoplasmic vacuoles (Figure 6F). These characteristics remained in the 12-hour period (data not shown). However, it was possible to identify evidence of nuclear fragmentation and degeneration in mitochondria after 24-hour treatment that was characterized by unpaired disrupted cristae. These changes were indicative of the beginning of the apoptotic process (Figure 6G-H).

MCF-7 cells were also treated with MIH 2.4BI at a higher dose of 75 μ M for 3, 6, 12, and 24 hours (Figure 7). Ultrastructural analysis of control and DMSO (vehicle)-treated MCF-7 cells showed similar morphologic characteristics described for the previous experiment (Figure 7A-D). There were also numerous roundish organelles, indicative of lysosomes containing very electron-dense, lamellar material present in both control and vehicle-treated cells. However, cells treated with MIH 2.4BI at a concentration of 75 μ M showed evidence of ultrastructural changes beginning at 3 hours after treatment compared with control or vehicle-treated cells, with alteration of nuclear morphology (Figure 7E) and mitochondrial degeneration (Figure 7F). These characteristics were also observed at 6 hours of treatment with MIH 2.4BI (data not shown). Beginning at 12 hours (Figure 7G) and continuing at 24 hours (Figure 7H), morphologic evidence indicating an advanced apoptotic state was present, which included nuclear fragmentation and degeneration of mitochondria, as well as numerous cytoplasmic vacuoles.

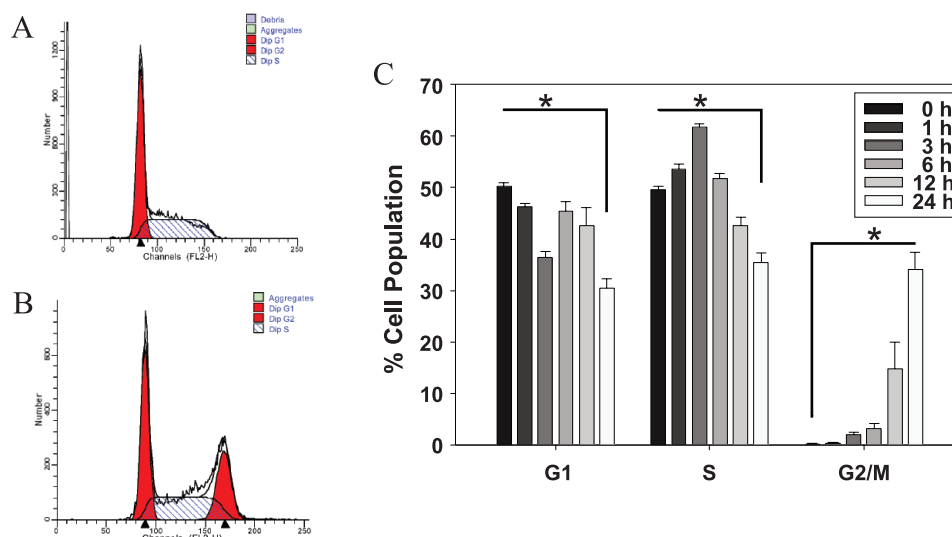


Figure 5. Effect of MIH 2.4BI on MCF-7 cell cycle distribution as determined by flow cytometry. (A) Histograms for cell cycle distribution of MCF-7 cells treated with DMSO (vehicle) alone. (B) Histograms for cell cycle distribution of MCF-7 cells treated with 75 μ M MIH 2.4BI for 24 hours. (C) Quantification of cell cycle distribution in MCF-7 cells treated with 75 μ M MIH 2.4BI for 0, 1, 3, 6, 12, or 24 hours. Results are presented as mean \pm SEM of data from 3 replicates. Compared between values at 0 and 24 hours, changes in % cell populations at G1, S, and G2/M were statistically different if $P < .05$ (*). DMSO indicates dimethyl sulfoxide.

To confirm that the morphologic changes observed by electron microscopy after treatment with MIH 2.4BI were mediated by apoptosis, TUNEL assays were performed. As shown in Figure 8, MCF-7 cells treated with 37.5 and 75 μ M MIH 2.4BI demonstrated positively stained nuclei (TUNEL) in a dose-dependent manner, which was indicative of DNA fragmentation occurring during the late event of apoptosis. In contrast, control (untreated) cells exhibited no evidence of DNA fragmentation. These data are supportive that treatment with MIH 2.4BI results in the induction of apoptosis in MCF-7 cells.

Discussion

Despite the existence of a considerable number of drugs for the treatment of cancer, in many cases, therapeutic success is not achieved due to treatment failures, resulting in high relapse rates, poor patient survival, and adverse effects; these outcomes necessitate a continuous search by new drugs.²⁹ Mesoionic compounds have received considerable attention and have been extensively studied because of their structures, reaction behavior, biological activities, and possible pharmaceutical use.^{30,31} We have described the synthesis of a new mesoionic compound, MIH 2.4BI. Cytotoxicity assays were performed to determine the potential anticancer activity of MIH 2.4BI in breast tumor cell lines, which demonstrated that the mesoionic compound inhibited most breast cancer cell lines, ranging from low to high activity.

In this study, we found that the MCF-7, T-47D, and ZR-75-1 cell lines exhibited a more potent sensitivity to growth inhibition by MIH 2.4BI compared with HMEC at 72 and 96 hours of treatment than the other breast cancer cell lines tested. Interestingly, these cell lines were derived from tumors

of luminal A origin, characterized by high expression of ER, PR, and HER2. Further studies will be needed to establish whether a correlation exists between the sensitivity to MIH 2.4BI and breast cancer subtypes. Nonetheless, luminal A is the most common subtype of human breast cancer, with the best prognosis.³² Conventional chemotherapeutic agents targeting cells of high proliferation index may not benefit luminal A patients.³³ Thus, MIH 2.4BI may prove more effective for this subtype. Likewise, it will be interesting to explore the cytotoxic effect of MIH 2.4BI in cancer stem cells, which have a low proliferation index.³⁴

We demonstrated from these experiments that MIH 2.4BI induced a cell cycle arrest at G2/M. Multiple mechanisms are mediated by anticancer agents in the induction of cell cycle arrest at G2/M, including inhibition of DNA replication, blockage of microtubule assembly/disassembly, and alkylation and crosslinking of DNA.³⁵ Further studies will be needed to understand the specific mechanism(s) of action of MIH 2.4BI to facilitate G2/M arrest. Cancer cells are often defective in cell cycle-checkpoint mechanisms,³⁶ which offer new opportunities for cancer treatment. Restoring proper checkpoint control to cancer cells might allow them to return to a quiescent state. Alternatively, new drugs targeting key regulators of the S and G2/M checkpoints are available to induce cytotoxicity and cell death.³⁷ It will be interesting to assess the potential combined effects of these agents with MIH 2.4BI in future studies.

The results of our electron microscopy analysis suggest a possible induction of death by mitochondrial dysfunction by the treatment with MIH 2.4BI, as demonstrated by evidence of mitochondrial degeneration. In support of these results, studies using the mesoionic compound SYD-1 in isolated rat liver mitochondria depressed the efficiency of electron transport

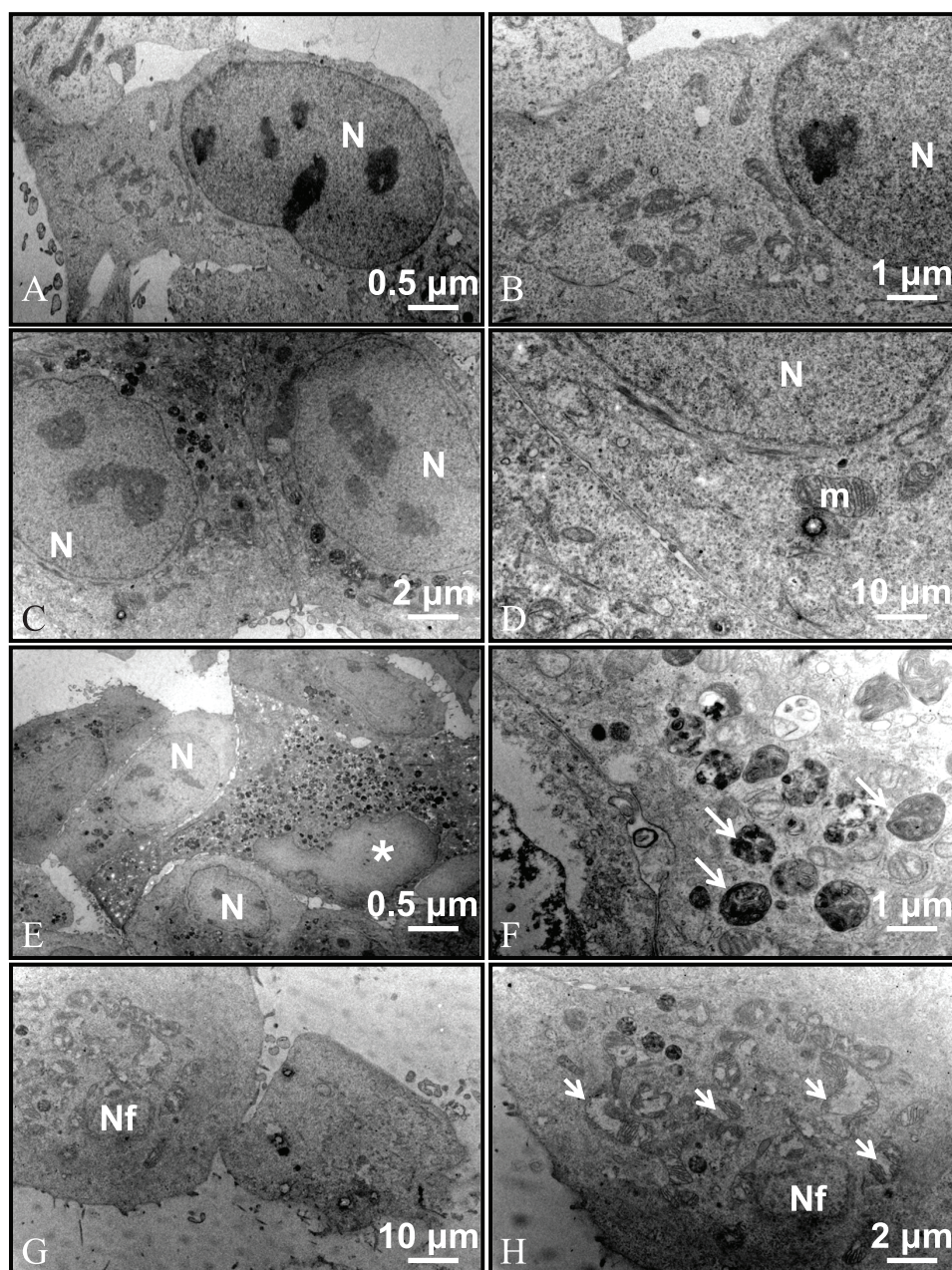


Figure 6. Transmission electron micrographs of MCF-7 cells treated with MIH 2.4BI at a concentration of 37.5 μ M. (A-B) Control (untreated) cells; (C-D) DMSO (vehicle)-treated cells; (E-F) treatment with MIH 2.4BI for 6 hours; (G-H) treatment with MIH 2.4BI for 24 hours. Arrowheads indicates mitochondrial degeneration; asterisk, nucleus with altered morphology; DMSO, dimethyl sulfoxide; long arrows, autophagic vacuoles; m, mitochondria; Nf, fragmented nucleus; N, nucleus.

and oxidative phosphorylation.³⁸ Another mesoionic compound, MI-D, was also shown to act as an uncoupler of the respiratory chain between complexes II and III.³⁹ Mechanistic studies demonstrated that alteration of membrane fluidity and elasticity were related to the disruption of mitochondrial function by mesoionic compounds.⁴⁰ Altered mitochondrial metabolism has been suggested as an approach to overcome the resistance to apoptosis in cancer cells.⁴¹ Future studies will be designed to further elucidate the mechanism(s) by which MIH 2.4BI could disrupt mitochondrial function.

In addition, our electron microscopy analysis revealed evidence of apoptosis, as demonstrated by alteration of the nuclear

morphology and numerous cytoplasmic vacuoles. The mechanism of apoptosis has been well described⁴² and characterized by morphological changes associated with cell death, including a diminution of cellular size, condensation and nuclear fragmentation, dynamic formation of membranes, loss of extracellular matrix and cell adhesion, and the formation of apoptotic bodies, which are phagocytosed by neighboring cells.⁴³ The biochemical alterations associated with apoptosis include cleavage of chromosomal DNA into internucleosomal fragments, phosphatidylserine externalization, and a number of intracellular substrate cleavages by specific proteolysis.⁴⁴ Our electron microscopy study indicated the type of cell death from

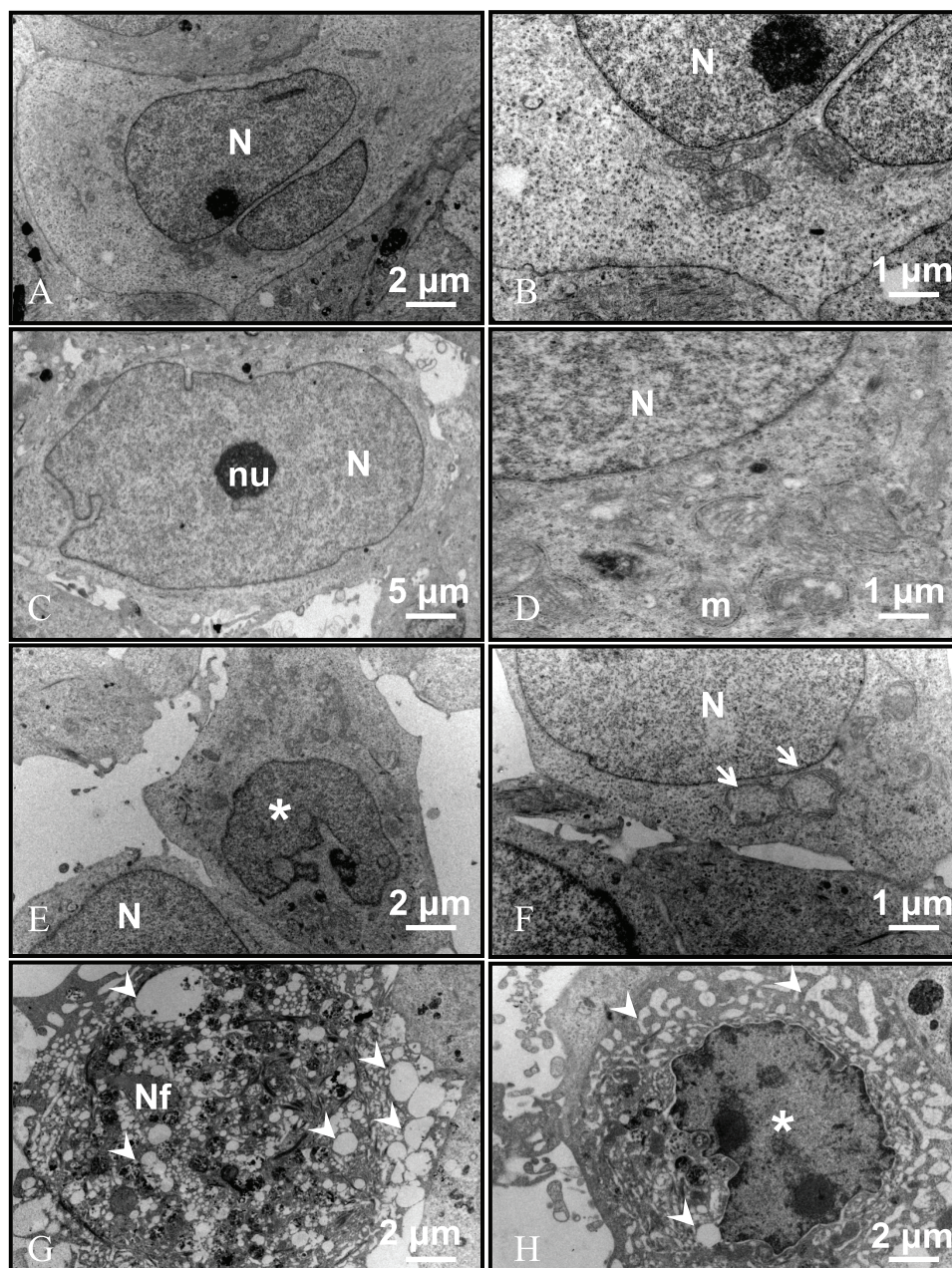


Figure 7. Transmission electron micrographs of MCF-7 cells treated with MIH 2.4BI at a concentration of 75 μ M. (A-B) Control (untreated) cells; (C-D) DMSO (vehicle)-treated cells; (E-F) treatment with MIH 2.4BI for 3 hours; (G) treatment with MIH 2.4BI for 12 hours; (H) treatment with MIH 2.4BI for 24 hours. Arrowheads indicates vacuoles; asterisk, nucleus with altered morphology; DMSO, dimethyl sulfoxide; long arrows, autophagic vacuoles; m, mitochondria; Nf, fragmented nucleus; N, nucleus, short arrows, mitochondrial degeneration.

treatment with MIH 2.4BI was likely mediated by apoptosis, a mechanism that was supported by our TUNEL assay results demonstrating DNA fragmentation occurring in the last phase of apoptotic cell death.

One of the advantages of inducing apoptosis as a form of cell death by chemotherapeutic agents is related to the fact that cells can be eliminated by the immune system without triggering an inflammatory response.⁴⁵ Our results corroborate with those reported by Senff-Ribeiro et al.⁴⁶ when studying the cytotoxic effects of 1,3,4-tetrazolium mesoionic compounds in melanoma cell lines, in which cellular alterations after

treatment were observed as apoptotic in nature demonstrated by a diminution of cell size and protuberance of apoptotic bodies. Understanding the mechanistic role of MIH 2.4BI in inducing apoptosis will be an important consideration of future studies.

The principle of designing new chemotherapy agents involves successive cycles of compound synthesis and testing, with each iteration yielding molecules that have improved characteristics over the previous set of compounds. To increase the efficacy of MIH 2.4BI, additional synthesis of structural analogs will be necessary to improve the IC_{50} values. In this

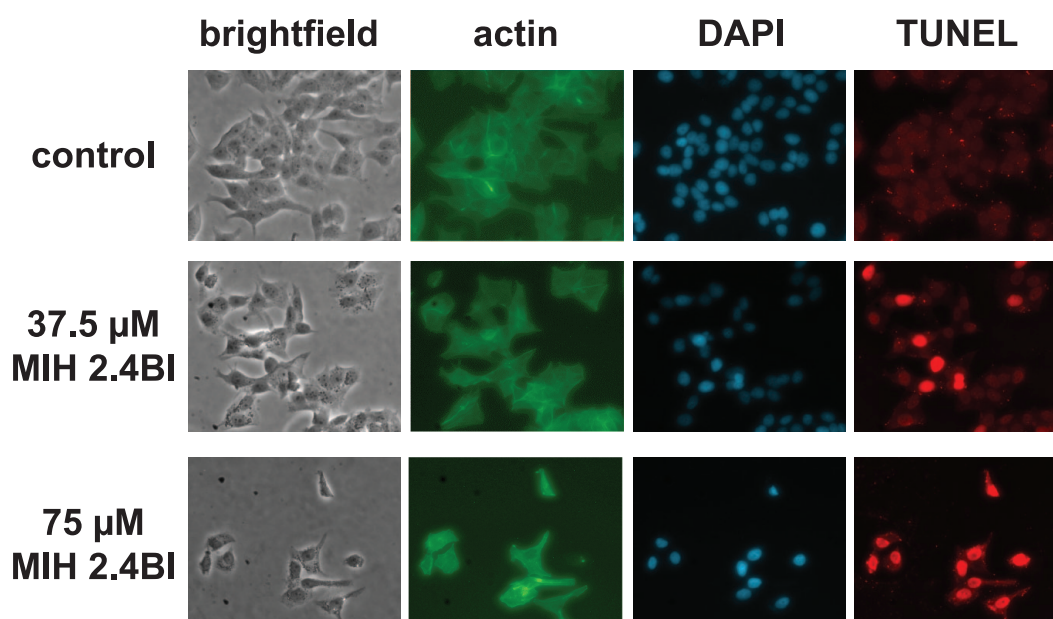


Figure 8. MIH 2.4BI induces apoptosis in MCF-7 cells. The cells were treated for 96 hours with MIH 2.4BI at a concentration of 37.5 or 75 μM and labeled using a Click-iT Plus EdU Alexa Fluor 594 Imaging Kit and compared with control (untreated) cells. TUNEL fluorescence was determined at an Ex/Em of 535 nm/580 nm (G-2A filter cube). DAPI fluorescence was determined at an Ex/Em of 375 nm/460 nm (DAPI filter cube). Actin fluorescence was determined at an Ex/Em of 470 nm/510 nm (B-2A filter cube). TUNEL indicates terminal deoxynucleotidyl transferase (TdT) deoxyuridine triphosphate (dUTP) nick end labeling; DAPI, 4',6-diamidino-2-phenylindole.

regard, substitutions of the 6-member heterocyclic ring structures of MIH 2.4BI with electron-withdrawing groups such as NO_2 may result in an increased positive charge on the mesoionic ring.⁴⁶ Based on the association of the mesoionic charge-pair system with biomolecules such as DNA and proteins,⁴⁷ these additional substitutions could dramatically affect the cytotoxic activity of MIH 2.4BI.⁴⁶ Although the mesoionic ring structure is internally charged, the charge-pair system is overall neutral allowing for the ability to cross biological membranes.⁴⁷ Also, the hydrophobic nature of the 6-member heterocyclic ring structures of MIH 2.4BI makes the compound a more hydrophobic molecule, likely allowing it to cross cell membranes more easily. Additional hydrophobic substitutions could enhance this effect. These considerations could be used to devise a future structure-activity relationship (SAR) study for designing and synthesizing new mesoionic compounds based on the initial structure of MIH 2.4BI.

The development and use of drug delivery systems is an important approach to improve the SI of a chemotherapy agent. The use of drug delivery systems has been largely unexplored in the case of mesoionic compounds. However, one example includes mesoporous silica nanoparticles, which have been studied as a platform for drug delivery due to their favorable properties, including biocompatibility, efficient cellular uptake, and controlled drug release.⁴⁸ In this regard, the mesoionic drug, molsidomine, was demonstrated to be capable of absorption onto different mesoporous silica materials.⁴⁹ In particular, absorption onto a phenyl-modified silica derivative was highest, likely due to the interaction between phenyl groups of the modified silica and the 6-member heterocyclic ring

structure of the molsidomine drug. Thus, it may be worthwhile in future studies to determine the uptake of MIH 2.4BI onto mesoporous silica nanoparticles as an approach to improve the specificity of intracellular uptake and release in cancer cells. In combination with targeting moieties such as peptides or other ligands, mesoporous silica nanoparticles have been a promising tool for drug delivery of cancer therapeutics.⁵⁰

In conclusion, we have demonstrated that the mesoionic compound MIH 2.4BI has anticancer activity in MCF-7 breast cancer cells of the luminal A subtype, resulting in the inhibition of cell growth and survival and induction of cell cycle arrest in the G2 phase. Electron microscopy and TUNEL data support a mechanism of action of cell death mediated by induction of apoptosis. However, further investigation is needed to elucidate the specific mechanistic pathways involved in inducing apoptotic cell death. Nonetheless, these studies confirm the potential therapeutic use of MIH 2.4BI in treating breast cancer.

Acknowledgements

The authors thank the research and administrative staff in the Department of Comparative Biomedical Science at the Louisiana State University School of Veterinary Medicine (United States) and the Federal Rural University of Pernambuco (Brazil) for their assistance.

Author Contributions

LAMC performed the experimental protocols, the analysis, and interpretation of the data. ACH assisted in designing and performing the apoptosis experiments and interpreting the results. FCSL assisted in performing the cell culture

experiments and interpreting the results. SSA and MMDM assisted in the statistical analysis of the data and interpretation of the results. AACT and FDP assisted in the design and performing of the electron microscopy experiments and in the analysis and interpretation of the data. HDSS synthesized the mesoionic compound used in the experiments. PFAF directed the synthesis of the mesoionic compound used in the experiments and interpreted the analysis of the results. SAJ, AW, and MAGF assisted in the design of the experimental methods and oversaw the analysis and interpretation of the data and writing of the article. JMM directed the project, designed the experimental protocols, oversaw the analysis and interpretation of the data, and writing of the article. All authors read and approved the final article.

Availability of Data and Materials

The data sets used and analyzed during the current study are available from the corresponding author on reasonable request.

ORCID iD

J Michael Mathis  <https://orcid.org/0000-0001-5528-5195>

REFERENCES

- Bray F, Ferlay J, Soerjomataram I, Siegel RL, Torre LA, Jemal A. Global cancer statistics 2018: GLOBOCAN estimates of incidence and mortality worldwide for 36 cancers in 185 countries. *CA Cancer J Clin*. 2018;68:394-424. doi:10.3322/caac.21492.
- DeSantis CE, Ma J, Goding Sauer A, Newman LA, Jemal A. Breast cancer statistics, 2017: racial disparity in mortality by state. *CA Cancer J Clin*. 2018;67:439-448. doi:10.3322/caac.214123.
- Albota F, Stanescu MD. The state of art in sydnonone chemistry and applications. *Rev Roum Chim*. 2017;62:711-734.
- Chandrasekhar R, Nanjan MJ. Sydnonones: a brief review. *Mini Rev Med Chem*. 2012;12:1359-1365. doi:10.2174/13895575112091359.
- Li Y, Geng J, Liu Y, Yu S, Zhao G. Thiadiazole—a promising structure in medicinal chemistry. *Chem Med Chem*. 2013;8:27-41. doi:10.1002/cmdc.201200355.
- Abdualkader AM, Taher M, Yusoff NIK. Mesoionic sydnone: a review in their chemical and biological properties. *Inter J Pharm*. 2017;9:1-9. doi:10.22159/ijpps.2017v9i8.18774.
- Senff-Ribeiro A, Echevarria A, Silva EF, Sanches Veiga S, Oliveira MB. Effect of a new 1,3,4-thiadiazolium mesoionic compound (MI-D) on B16-F10 murine melanoma. *Melanoma Res*. 2003;13:465-471.
- Senff-Ribeiro A, Echevarria A, Silva EF, Franco CR, Veiga SS, Oliveira MB. Cytotoxic effect of a new 1,3,4-thiadiazolium mesoionic compound (MI-D) on cell lines of human melanoma. *Br J Cancer*. 2004;91:297-304.
- Dunkley CS, Thoman CJ. Synthesis and biological evaluation of a novel phenyl substituted sydnone series as potential antitumor agents. *Bioorg Med Chem Lett*. 2003;13:2899-2901.
- Gozzi GJ, Pires Ado R, Martinez GR, et al. The antioxidant effect of the mesoionic compound SYD-1 in mitochondria. *Chem Biol Interact*. 2013;205:181-187.
- Galuppo LF, dos Reis Livero FA, Martins GG, et al. Sydnone 1: a mesoionic compound with antitumoral and haematological effects in vivo. *Basic Clin Pharmacol Toxicol*. 2016;119:41-50.
- Peixoto IN, Souza HDS, Lira BF, et al. Synthesis and antifungal activity against candida strains of mesoionic system derived from 1,3-thiazolium-5-thiolate. *J Brazilian Chem Soc*. 2016;27:1807-1813. doi:10.5935/0103-5053.20160063.
- Barbosa-Silva R, Nogueira MA, Souza HD, Lira BF, de Athayde-Filho PF, de Araújo CB. First hyperpolarizability of 1, 3-thiazolium-5-thiolates mesoionic compounds. *J Phy Chem C*. 2018;123:677-683.
- Lira BF, de Athayde Filho PF, Miller J, Simas AM, De Farias Dias A, Vieira MJ. Synthesis and characterization of some new mesoionic 1, 3-thiazolium-5-thiolates via cyclodehydration and in situ 1, 3-dipolarcycloaddition/cycloreversion. *Molecules*. 2002;7:791-800.
- Smith SE, Mellor P, Ward AK, et al. Molecular characterization of breast cancer cell lines through multiple omic approaches. *Breast Cancer Res*. 2017;19:65.
- Feoktistova M, Geserick P, Leverkus M. Crystal violet assay for determining viability of cultured cells. *Cold Spring Harb Protoc*. 2016;pdb.prot087379. doi:10.1101/pdb.prot087379.
- Tsou SH, Chen TM, Hsiao HT, Chen YH. A critical dose of doxorubicin is required to alter the gene expression profiles in MCF-7 cells acquiring multidrug resistance. *PLoS ONE*. 2015;10:e0116747.
- Jokar F, Mahabadi JA, Salimian M, et al. Differential expression of HSP90β in MDA-MB-231 and MCF-7 cell lines after treatment with doxorubicin. *J Pharmacopuncture*. 2019;22:28-34.
- Fornari FA, Randolph JK, Yalowich JC, Ritke MK, Gewirtz DA. Interference by doxorubicin with DNA unwinding in MCF-7 breast tumor cells. *Mol Pharmacol*. 1994;45:649-656.
- Mea Crowley LC, Chojnowski G, Waterhouse NJ. Measuring the DNA content of cells in apoptosis and at different cell-cycle stages by propidium iodide staining and flow cytometry. *Cold Spring Harb Protoc*. 2016;2016:10. doi:10.1101/pdb.prot08724701.
- Lee AV, Oesterreich S, Davidson NE. MCF-7 cells—changing the course of breast cancer research and care for 45 years. *J Natl Cancer Inst*. 2015;107:djv073.
- Comşa Ş, Cimpean AM, Raica M. The story of MCF-7 breast cancer cell line: 40 years of experience in research. *Anticancer Res*. 2015;35:3147-3154.
- Anvar SY, Allard G, Tseng E, et al. Full-length mRNA sequencing uncovers a widespread coupling between transcription initiation and mRNA processing. *Genome Biol*. 2018;19:46.
- Chiang YS, Huang YF, Midha MK, Chen TH, Shiau HC, Chiu KP. Single cell transcriptome analysis of MCF-7 reveals consistently and inconsistently expressed gene groups each associated with distinct cellular localization and functions. *PLoS ONE*. 2018;13:e0199471.
- Scudiero DA, Shoemaker RH, Paull KD, et al. Evaluation of a soluble tetrazolium/formazan assay for cell growth and drug sensitivity in culture using human and other tumor cell lines. *Cancer Res*. 1988;48:4827-4833.
- Śliwka L, Wiktorska K, Suchocki P, et al. The comparison of MTT and CVS assays for the assessment of anticancer agent interactions. *PLoS ONE*. 2016;11:e0155772.
- Fouche G, Cragg GM, Pillay P, Kolesnikova N, Maharaj VJ, Senabe J. In vitro anticancer screening of South African plants. *J Ethnopharmacol*. 2008;3:455-461.
- Suffness M, Pezzuto JM. Assays related to cancer drug discovery. In: Hostettmann K, ed. *Methods in Plant Biochemistry: Assay for Bioactivity*. London, England: Academic Press; 1990:71-133.
- Tang Y, Wang Y, Kiani MF, Wang B. Classification, treatment strategy, and associated drug resistance in breast cancer. *Clin Breast Cancer*. 2016;16:335-343.
- Kaur G, Singh R. Thiadiazole analogs as potential pharmacological agents: a brief review. *Int J Pharm Sci*. 2014;6:35-46.
- Abdualkader AM, Taher MU, Yusoff NI. Mesoionic sydnonones. A review in their chemical and biological properties. *Int J Pharm Pharm Sci*. 2017;9:1-9.
- Veronesi U, Boyle P, Goldhirsch A, Orecchia R, Viale G. Breast cancer. *Lancet*. 2005;365:1727-1741.
- Nielsen TO, Jensen M-B, Burugu S, et al. High-risk premenopausal luminal a breast cancer patients derive no benefit from adjuvant cyclophosphamide-based chemotherapy: results from the DBCG77B Clinical Trial. *Clin Cancer Res*. 2017;23:946-953.
- Munoz P, Iliou MS, Esteller M. Epigenetic alterations involved in cancer stem cell reprogramming. *Mol Oncol*. 2012;6:620-636.
- Barnum KJ, O'Connell MJ. Cell cycle regulation by checkpoints. In: Noguchi E, Gadaleta M, eds. *Cell Cycle Control. Methods in Molecular Biology (Methods and Protocols)*, vol 1170. New York, NY: Humana Press;2014. doi:10.1007/978-1-4939-0888-2_2.
- Foster I. 2008 Cancer: a cell cycle defect. *Radiography*;14:144-149. doi:10.1016/j.radi.2006.12.001.
- Visconti R, Della Monica R, Grieco D. Cell cycle checkpoint in cancer: a therapeutically targetable double-edged sword. *J Exp Clin Cancer Res*. 2016;35:153.
- Halila GC, de Oliveira MBM, Echevarria A, et al. Effect of sydnone SYD-1, a mesoionic compound, on energy-linked functions of rat liver mitochondria. *Chem Biol Interact*2007;169:160-170.
- Cadena SMSC, Carnieria EGS, Echevarria E, de Oliveira MBM. Effect of MI-D, a new mesoionic compound, on energy-linked functions of rat liver mitochondria. *FEBS Lett*. 1998;440:46-50.
- Cadena SM, Carnieri EG, Echevarria A, de Oliveira MB. Interference of MI-D, a new mesoionic compound, on artificial and native membranes. *Cell Biochem Funct*. 2002;20:31-37.
- Vyas S, Zaganjor E, Haigis MC. Mitochondria and cancer. *Cell*. 2016;166:555-566.
- D'Arcy MS. Cell death: a review of the major forms of apoptosis, necrosis and autophagy. *Cell Biol Int*. 2019;43:582-592.

43. Arandjelovic S, Ravichandran KS. Phagocytosis of apoptotic cells in homeostasis. *Nat Immunol.* 2015;16:907-917.
44. Pfeffer CM, Singh AT. Apoptosis: a target for anticancer therapy. *Int J Mol Sci.* 2018;19:448.
45. Wong RSY. Apoptosis in cancer: from pathogenesis to treatment. *J Exp Clin Cancer Res.* 2011;30:87.
46. Senff-Ribeiro A, Echevarria A, Silva EF, Veiga SS, Oliveira MB. Antimelanoma activity of 1,3,4-thiadiazolium mesoionics: a structure-activity relationship study. *Anticancer Drugs.* 2004;15:269-275.
47. Kier LB, Roche EB. Medicinal chemistry of the mesoionic compounds. *J Pharm Sci.* 1967;56:149-168.
48. Slowing II, Vivero-Escoto JL, Wu CW, Lin VS. Mesoporous silica nanoparticles as controlled release drug delivery and gene transfection carriers. *Adv Drug Deliv Rev.* 2008;60:1278-1288.
49. Alyoshina NA, Parfenyuk EV. Effect of surface properties of mesoporous silica on adsorption of mesoionic compound molsidomine. *J Mat Res.* 2012;27:2858-2866.
50. Watermann A, Brieger J. Mesoporous silica nanoparticles as drug delivery vehicles in cancer. *Nanomaterials.* 2017;7:189.